3310–3317 *Nucleic Acids Research, 1999, Vol. 27, No. 16*

Site-directed mutagenesis of motif III in PcrA helicase reveals a role in coupling ATP hydrolysis to strand separation

Mark S. Dillingham, Panos Soultanas and Dale B. Wigley*

Sir William Dunn School of Pathology, University of Oxford, South Parks Road, Oxford OX1 3RE, UK

Received May 4, 1999; Revised and Accepted June 9, 1999

ABSTRACT

Motif III is one of the seven protein motifs that are characteristic of superfamily I helicases. To investigate its role in the helicase mechanism we have introduced a variety of mutations at three of the most conserved amino acid residues (Q254, W259 and R260). Biochemical characterisation of the resulting proteins shows that mutation of motif III affects both ATP hydrolysis and single-stranded DNA binding. We propose that amino acid residue Q254 acts as a γ-phosphate sensor at the nucleotide binding pocket transmitting conformational changes to the DNA binding site, since the nature of the charge on this residue appears to control the degree of coupling between ATPase and helicase activities. Residues W259 and R260 both participate in direct DNA binding interactions that are critical for helicase activity.

INTRODUCTION

DNA helicases are ubiquitous enzymes involved in almost all aspects of DNA metabolism. They hydrolyse ATP and use the associated free energy change to translocate along the DNA duplex and separate the annealed strands (for reviews see 1,2). A central question in the enzymology of DNA helicases is understanding the manner in which the energy produced by ATP hydrolysis is coupled to the helicase function. Wong and Lohman (3) have demonstrated that the Rep helicase of *Escherichia coli* is an allosteric enzyme, whose DNA binding properties are modulated by the binding and hydrolysis of ATP. More recently, structural studies on PcrA helicase have provided further insight into the coupling mechanism.

The *Bacillus stearothermophilus* PcrA helicase is a member of helicase superfamily I and is highly homologous to the Rep and UvrD helicases of *E.coli* (4). The enzyme has been cloned and biochemically characterised in our laboratory (5). The crystal structures of this helicase alone and in complex with ADP have been solved at 2.5 and 2.9 Å, respectively (6). More recently, the enzyme has been co-crystallised with a tailed duplex DNA and either adenylylimido diphosphate (AMP-PNP) or a sulphate ion (7). AMP-PNP is a non-hydrolysable analogue of ATP and therefore the PcrA–DNA–AMP-PNP complex mimicks the nucleotide-bound state of PcrA before hydrolysis, a 'substrate' complex. The positioning of the sulphate ion in the PcrA–DNA–SO_4^{2-} complex mimicks the inorganic phosphate ion after hydrolysis, to represent a 'product' complex. These 'substrate' and 'product' complexes have been solved at 3.3 and 2.9 Å, respectively (7; Fig. 1). Together, the four structures provide clues as to how the free energy associated with ATP hydrolysis may be coupled to DNA strand separation.

Motif III is one of seven conserved 'helicase signature motifs' in superfamily I DNA helicases which are all found clustered around the nucleotide binding pocket (6). Previous mutagenesis studies on motif III in *E.coli* UvrD helicase have produced proteins displaying low processivity (8) and an inability to initiate unwinding from a nick (9), suggesting that motif III forms an interface between the ATPase and DNA binding domains. Analysis of the crystal structures of PcrA reveals that motif III forms a loop that connects the nucleotide binding pocket and the single-stranded DNA (ssDNA) binding site (Fig. 1). In the structures of the 'substrate' and 'product' complexes of PcrA (7) a conserved glutamine residue from motif III (Q254) directly contacts the γ-phosphate of AMP-PNP and the sulphate ion, respectively (Fig. 1), implying that this residue contacts the γ-phosphate of ATP before and after hydrolysis. This contact would be lost on P_i release. The structures also show that conserved tryptophan and arginine residues from motif III (W259 and R260) make direct ssDNA contacts (Fig. 1). The equivalent residues in the *E.coli* Rep helicase make similar ssDNA contacts in the structure of this enzyme in complex with ssDNA (10)

Further evidence that motif III may couple ATP hydrolysis to the DNA binding properties of PcrA comes from structural comparison with the RecA protein of *E.coli*, which plays a central role in the process of homologous recombination. The 1A and 2A domains of PcrA have the same protein fold as the ATP binding domain of RecA protein (6,11). Importantly, this similarity extends to the nucleotide binding pocket, where amino acids are found to be highly spatially conserved (Fig. 2A), despite the fact that the two proteins display no apparent sequence homology. This observation raises the possibility that PcrA and RecA may employ similar mechanisms in aspects of their enzyme function. In the light of the crystal structure of the RecA–ADP complex, Story and Steitz (11) proposed a switch-like coupling mechanism between ATP binding and alterations in the ssDNA binding affinity of RecA. In their model, the disordered loop region L2

*To whom correspondence should be addressed. Tel: +44 1865 285479; Fax: +44 1865 275515; Email: wigley@eric.path.ox.ac.uk

The authors wish it to be known that, in their opinion, the first two authors should be regarded as joint First Authors

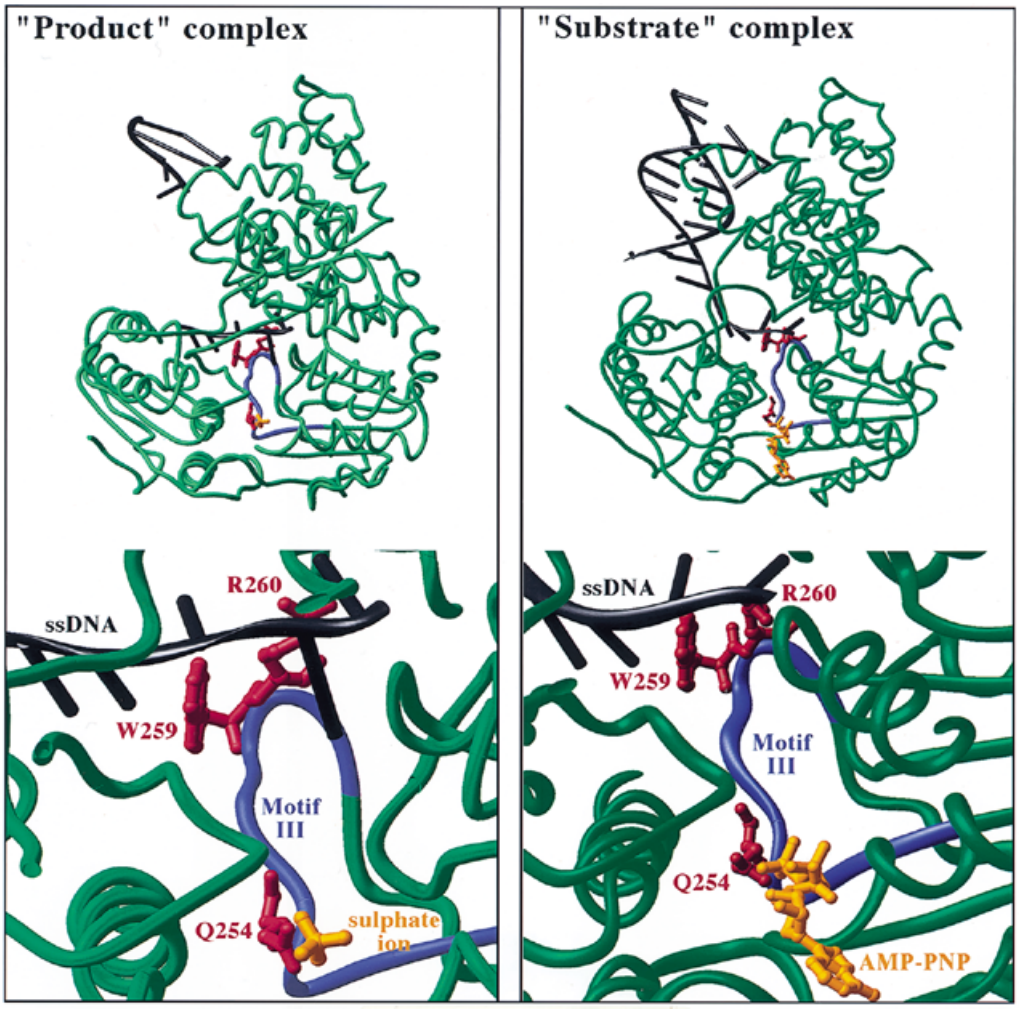

Figure 1. Crystal structures of 'product' and 'substrate' complexes of PcrA helicase (7). In both cases the conserved protein motif III is shown in blue, with residues selected for mutagenesis (Q254, W259 and R260) shown in red. The sulphate ion and AMP-PNP are shown in gold. The tailed duplex DNA is shown in black with the phosphodiester backbones and bases represented as ribbons and cylinders, respectively. Below each structure is a close-up of motif III which shows how it bridges the nucleotide binding site and the ssDNA binding site. Trp259 and Arg260 make direct ssDNA contacts in both structures. Gln254 contacts the sulphate ion and the γ-phosphate of AMP-PNP in the 'product' and 'substrate' complexes, respectively.

played a role analogous to that of the switch II region of the ras p21 protein (12), modulating allosteric transitions in response to ATP binding and hydrolysis. They suggested that a conserved glutamine in the nucleotide binding pocket (Q194) would interact with the γ-phosphate of ATP and stabilise high affinity ssDNA binding by the L2 loop. Their idea is supported by recent mutagenesis studies (13). In PcrA the motif III loop is the structural equivalent of loop L2 of RecA. Moreover, Q254 of motif III contacts the nucleotide binding pocket at the same position as does Q194 of loop L2 (6; Fig. 2A). These observations suggested to us that the DNA helicases may also employ a switch-like mechanism to couple the free energy change of NTP hydrolysis to helicase activity and implicated the motif III loop as a good candidate for such a role. A model to explain how motif III may contribute to the allosteric regulation of PcrA in response to ATP binding and hydrolysis is summarised in diagrammatic form in Figure 2B.

To test this model we used site-directed mutagenesis to alter three of the conserved motif III residues (Q254, W259 and R260, as indicated in Fig. 1) and characterised the biochemical properties of the resulting mutant PcrA proteins. Our results indicate that motif III plays a critical role in coupling ATPase and helicase activities since alterations in this protein signature lead to defects in both ATP hydrolysis and ssDNA binding. It includes both a γ-phosphate sensor at the nucleotide binding pocket (residue Q254) and a part of the DNA binding apparatus which is critical for helicase activity (residues W259 and R260). These studies extend our understanding of the mechanism of allosteric regulation of superfamily I DNA helicases and confirm the similarity between PcrA and RecA in this respect.

MATERIALS AND METHODS

Site-directed mutagenesis of the *pcrA* gene

Site-directed mutagenesis was carried out by 'splicing by overlap extension' as described elsewhere (14). The PCR programme used for the first and second step reactions was: 14

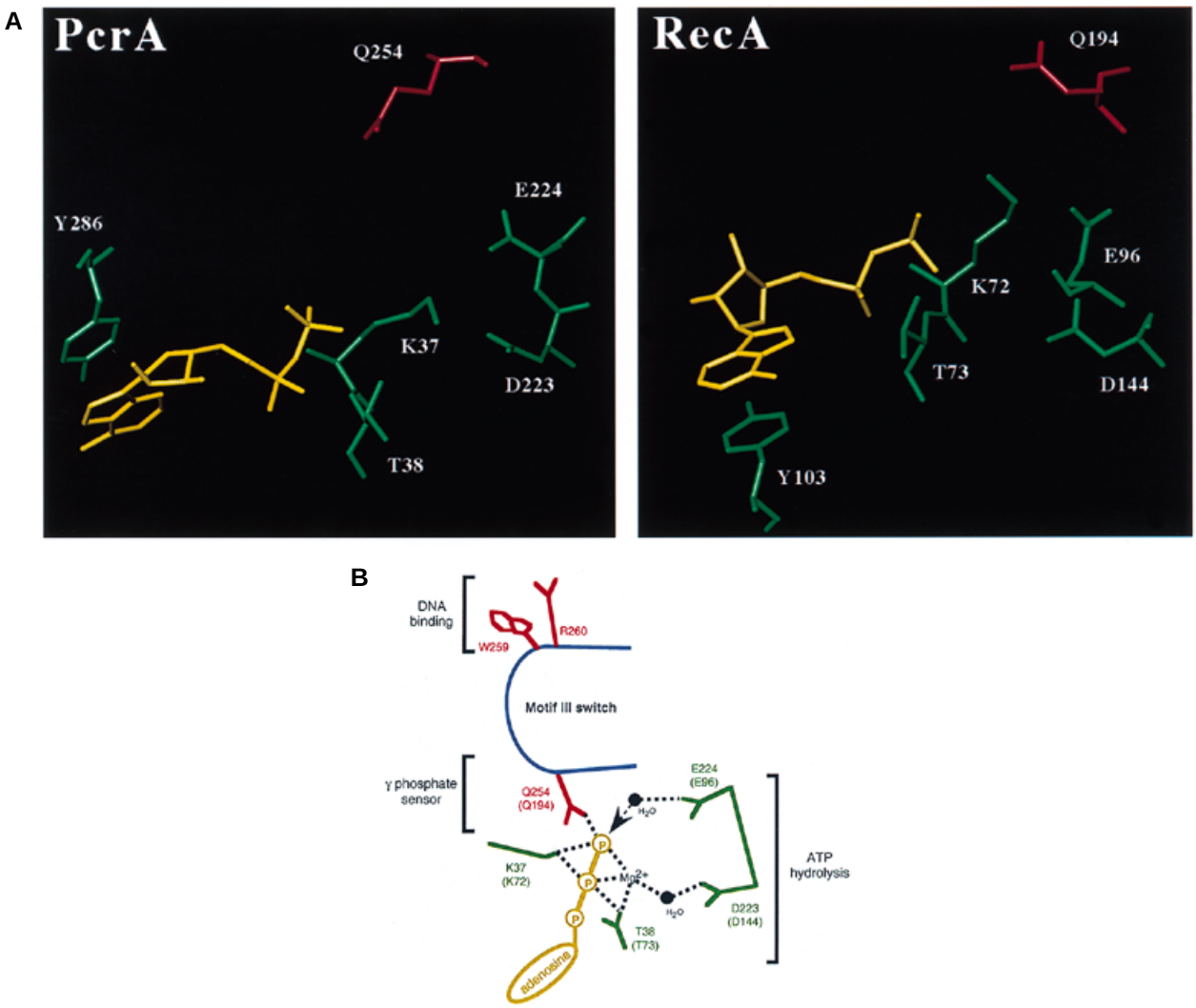

Figure 2. (**A**) A comparison of the nucleotide binding pockets of PcrA (left) and RecA (right), both complexed with ADP. The conserved glutamine residues of interest are shown in red. The structures reveal a high degree of spatial conservation around the bound nucleotide. The RecA figure was created by overlaying coordinates for the bound ADP (PDB accession no. 1REA) on coordinates for the apo-enzyme (PDB accession no. 2REB), since complete coordinates for the RecA–ADP complex are not available. (**B**) Proposed mechanism for allosteric coupling of ATP binding and hydrolysis to DNA binding and helicase activity via an 'on–off' switch in PcrA helicase motif III. Transient interaction of Q254 of motif III with the γ-phosphate of ATP modifies the DNA binding site formed by W259 and R260 of the same motif. The colour scheme of the previous two figures is maintained. The diagram is based on a similar figure which appeared in a report of the structure of the RecA–ADP complex (11). The ATP binding domains of PcrA and RecA share the same structural fold and residues in their nucleotide binding pockets are spatially conserved. The equivalent residues in RecA are shown in brackets. Residues K37 and T38 of motif I and D223 and E224 of motif II are assumed to be functionally equivalent to their RecA counterparts. This assumption is supported by mutagenesis studies in PcrA (22).

cycles of 94°C for 70 s, 58°C for 40 s and 72°C for 80 s and a final extension step at 72°C for 4 min. The reactions were done with the Expand™ high fidelity PCR system (Boehringer Mannheim) in a total reaction volume of 50 µl at 1.5 mM $MgCl_2$ using 100 ng of substrate DNA and 500 ng of each primer. All other reaction conditions were as described by the manufacturer.

The final PCR reaction products carrying the appropriate mutations were gel purified and then cut with suitable restriction endonucleases (*Nru*I and *Hin*dIII). The restriction fragments carrying the mutations were then used to replace the equivalent fragments in the *pcrA* gene. Successful mutants were primarily selected by detecting the appearance or abolition of a restriction site (W259A creates a *Sac*II site, R260A creates a *Bcn*I site, all Q254 mutations destroy a unique *Cla*I site). All mutants were sequenced to verify the mutations and the absence of spurious mutations which might have been introduced by the PCR reactions.

Protein purification

Wild-type and mutant proteins (with the exception of Q254K PcrA) were purified in a similar manner to that described previously (15). Minor alterations in the purification procedure were used in the case of the Q254K protein, full details of

which can be found in the same reference. Unexpectedly, the Q254K mutant protein was found to be toxic to *E.coli* B834 cells and had to be expressed in B834 cells containing the pLysS plasmid, which tightly controls expression until induction. Since the mutant protein was also found to be less soluble than wild-type PcrA, we included 2% Triton X-100 and higher salt (1 M) in our cell lysis buffer.

ATPase assays

ATPase activity was assayed by linking ATP hydrolysis to the oxidation of NADH as described previously (16). The reactions were carried out in 20 mM Tris pH 7.5, 50 mM NaCl, 3 mM $MgCl_2$, 4 mM DTT and contained either 24 or 120 nM protein in the presence or absence of saturating synthetic oligo$(dT)_{16}$ (50-fold molar excess over protein or 3000-fold for the W259A mutant). Values for the Michaelis–Menten constants k_{cat} and K_m for ATP were derived by fitting data directly to the Michaelis–Menten equation (GraphPad Prism 2.0). Several independent experiments were performed for each mutant in which ATP concentration was varied at least 5-fold above and below the measured K_m.

The dependence of the rate of the ATPase reaction on ssDNA cofactor was examined with the method above in a buffer containing 50 mM Tris–acetate pH 7.5, 0.1 mM EDTA, 10 mM $MgCl_2$ and 0.1 mg/ml BSA and using 2 mM (saturating) ATP and 24 nM protein in the presence of various quantities of synthetic oligo$(dT)_{16}$. The data were fitted directly to the Michaelis–Menten equation (GraphPad Prism 2.0) and this was used to compare the relative ability of the PcrA proteins to bind ssDNA. The term K_{DNA} is defined as the concentration of ssDNA required to achieve half-maximal stimulation of ATP hydrolysis under these assay conditions.

Background values for ATP hydrolysis in the absence of protein were <5% of the lowest experimental values determined (<0.05% of the highest) and were deducted as appropriate.

Helicase assays

A 3'-tailed substrate for helicase assays was prepared by annealing a radioactively labelled synthetic oligonucleotide to a slight excess of ssM13mp18 DNA as described previously (17). Helicase time course reactions were carried out at 37°C in a reaction buffer containing 20 mM Tris pH 7.5, 50 mM NaCl, 3 mM $MgCl_2$, 2.5 mM ATP, 4 mM DTT (the same buffer as was used for ATP hydrolysis assays) and 10% glycerol using 0.6 μM protein and 1 nM DNA substrate. After a 2 min preincubation the reactions were started with protein and later stopped by adding stop buffer (0.4% w/v SDS, 40 mM EDTA, 8% v/v glycerol, 0.1% w/v bromophenol blue). Protein titration experiments were performed exactly as above but using various quantities of protein and 5 min at 37°C as the incubation time for the reaction.

Displaced oligonucleotide was separated from annealed oligonucleotide by electrophoresis through a 10% non-denaturing polyacrylamide mini-gel at constant voltage (150 V). Gels were then dried and exposed to X-ray film as appropriate. Quantitative analysis was performed with a phosphorimager and ImageQuant software (Molecular Dynamics). Approximate comparisons between wild-type and mutant helicase rates were made by fitting initial rate lines to the first time point in each series.

Nitrocellulose filter binding assay

Nitrocellulose filter binding assays were performed using a 96-well dot blot apparatus (Flowgen). Filters were prepared by soaking BioBond NC nitrocellulose membranes (Whatman) in 0.4 M KOH for 30 min followed by several washes in distilled H_2O until the pH was equal to 7. Filters were then equilibrated in binding buffer (20 mM Tris pH 7.5, 50 mM NaCl, 3 mM $MgCl_2$, 4 mM DTT, 10% glycerol) for 1 h prior to use. Reaction mixtures (20 μl) contained binding buffer, 0.1 pmol radiolabelled synthetic oligo$(dT)_{16}$ and various quantities of protein. Incubations were performed at room temperature for 20 min. Immediately before filtering the samples, each well was flushed with 200 μl of binding buffer. Samples were then applied to the filter under suction and the wells were immediately washed with a further 200 μl binding buffer. Filters were then removed, air dried and DNA retention was calculated using a phosphorimager and ImageQuant software (Molecular Dynamics). Background values for the retention of probe in the absence of PcrA were always <2% of full retention.

Electrophoretic mobility shift assays

Further analysis of ssDNA binding was performed using the electrophoretic mobility shift assay technique. Protein, at various concentrations, was incubated with 2.5 nM single-stranded 45mer (the same oligonucleotide as was used to make the helicase substrate) in the same buffer used for helicase assays at room temperature for 20 min. The samples were then run on a 10% native polyacrylamide gel to separate the protein–DNA complex from the free DNA. Gels were dried and exposed to X-ray film.

RESULTS

W259A and R260A mutants of PcrA display ssDNA binding defects

The ATPase activity of PcrA is dependent upon ssDNA as a cofactor. This property was used as an indirect measure of the ability of the mutant enzymes to bind ssDNA. Both mutants required higher levels of ssDNA than the wild-type enzyme to achieve maximal stimulation of ATP hydrolysis (Fig. 3 and Table 1). The W259A mutant displayed a severe defect requiring a 200-fold higher concentration of ssDNA to achieve half-maximal ATPase stimulation (Fig. 3 and Table 1). This ssDNA binding defect of the W259A mutant was readily detectable using nitrocellulose filter binding and gel shift techniques (Fig. 4A and B). The R260A mutation produced a protein with a mild defect requiring only 3.5-fold more ssDNA to achieve half-maximal ATPase stimulation (Fig. 3 and Table 1). The defect was too small to be detected clearly either by nitrocellulose filter binding studies (Fig. 4A) or gel shifts (Fig. 4B).

W259A and R260A mutants display wild-type ATPase activity but are poor helicases

In the presence of saturating ssDNA, the W259A and R260A PcrA proteins displayed near wild-type k_{cat} and K_m values for ATP hydrolysis (Table 1).

The W259A and R260A mutations produce proteins with poor helicase activities (Fig. 5A). The W259A protein was only capable of catalysing helicase activity marginally above

Table 1. Kinetic analysis of steady-state ATP hydrolysis in wild-type and mutant PcrA proteins

Protein	k_{cat} (s^{-1})	k_{cat} decrease factor	K_m (μM)	K_m (wt)/K_m (mut)	(k_{cat}/K_m) × 1000	K_{DNA} (μM)
Wild-type	11.0	1	56	1	200	0.13
Q254E	1.24	8.9	27	2.1	40	Nd
Q254A	0.37	30	1.8	30	200	Nd
Q254N	0.15	70	18	3.1	8	Nd
Q254R	0.11	100	56	1.0	2	Nd
Q254K	0.29	38	63	0.89	5	Nd
W259A	10.4	1.1	54	1.0	190	28
R260A	5.2	2.1	35	1.6	150	0.46

Nd, not determined.

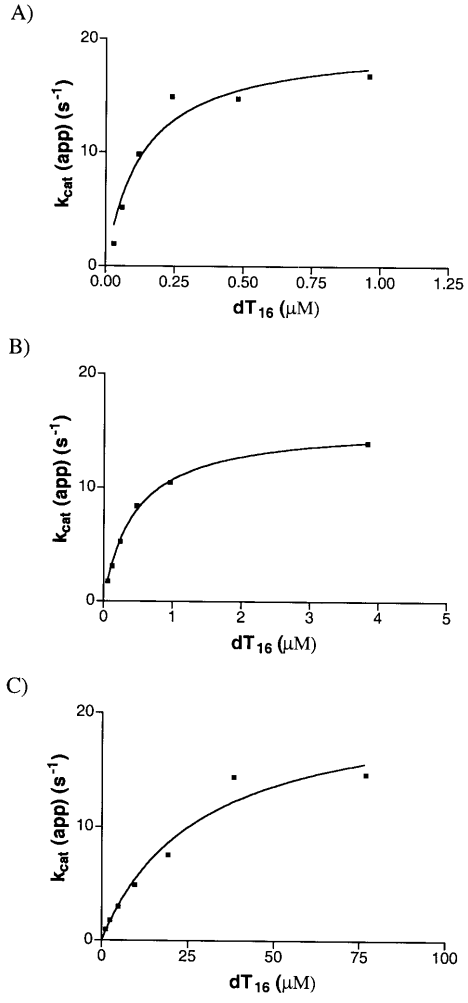

Figure 3. Single-stranded DNA stimulation of ATPase activity in (**A**) wild-type, (**B**) R260A and (**C**) W259A PcrA. Rates of ATP hydrolysis were determined at various ssDNA concentrations in the presence of saturating quantities of ATP as described in Materials and Methods. Values for K_{DNA} (defined in Materials and Methods) were derived by fitting these data directly to the Michaelis–Menten equation and are shown in Table 1.

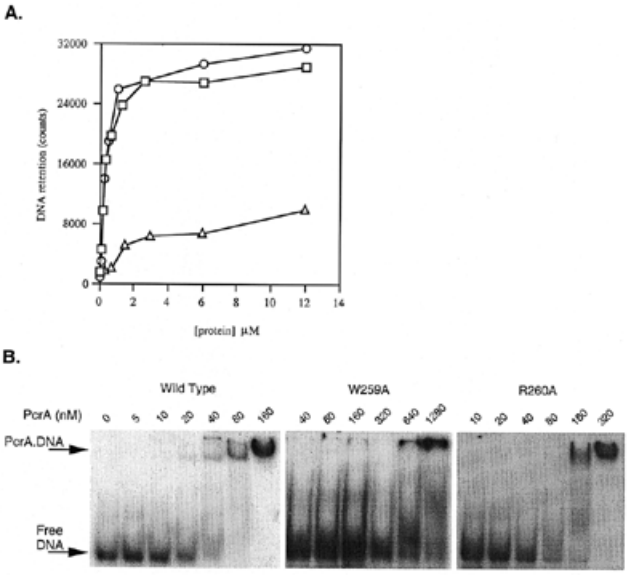

Figure 4. DNA binding by wild-type, W259A and R260A PcrA. (**A**) Nitrocellulose filter binding assays. Wild-type (square), R260A (circle) and W259A (triangle) PcrA at various concentrations were incubated with 5 nM radiolabelled oligo(dT)$_{16}$. All samples were then loaded onto the same filter to separate the bound DNA which was quantified using a phosphorimager and ImageQuant software (Molecular Dynamics). (**B**) Electrophoretic mobility shift assays. Wild-type, R260A and W259A PcrA at the concentrations shown were incubated with 2.5 nM radiolabelled ssDNA (45mer) in a standard buffer. The samples were then run on a 10% native polyacrylamide gel to separate the protein–DNA complex from the free DNA. Further details of both experiments are described in Materials and Methods.

background levels. The rate of oligonucleotide displacement by W259A was around 300-fold slower than that of wild-type PcrA. Although the R260A PcrA was able to produce some activity, this was still substantially (~90-fold) below that of wild-type PcrA. Since both of these mutations resulted in ssDNA binding defects we decided to investigate whether it is possible to 'recover' wild-type helicase rates simply by working at higher protein concentrations. In the case of the R260A mutant, the magnitude of oligonucleotide displacement after 5 min remained at <50%, even at protein concentrations two orders of magnitude above that required for >90% displacement in wild-type PcrA (Fig. 5B). In the case of the W259A mutant, helicase activity is very low and is not increased noticeably by the addition of larger amounts of protein to the reaction mixture (Fig. 5B).

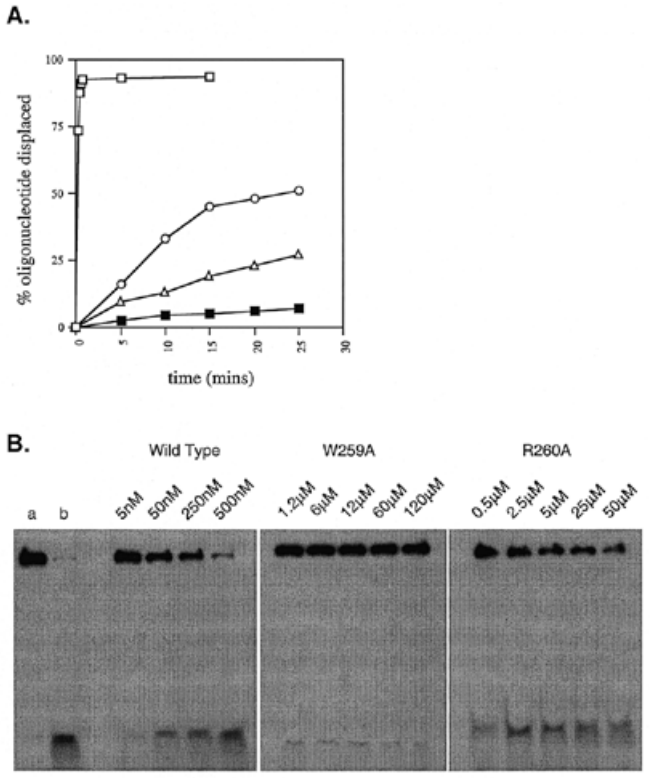

Figure 5. Comparative helicase assays for wild-type, W259A and R260A PcrA. (**A**) Helicase time course assays for wild-type (open square), W259A (triangle) and R260A (circle) PcrA. A control assay for wild-type PcrA in the absence of ATP is also shown (filled square). Reactions were performed with 0.6 μM protein and 1 nM DNA substrate. Annealed and displaced oligonucleotides were separated by electrophoresis through a 10% non-denaturing polyacrylamide gel and quantified using a phosphorimager and ImageQuant software (Molecular Dynamics). (**B**) Single time point protein titration helicase assays. Lane a shows oligonucleotide annealed to ssM13mp18 after incubation at 37°C for 5 min and represents a no protein control. Lane b shows oligonucleotide displaced from ssM13mp18 by boiling for 10 min prior to loading. Helicase assays were performed for 5 min using 1 nM DNA substrate and various protein concentrations (indicated above each lane) as described in Materials and Methods.

All mutations at Q254 in PcrA reduce ATPase activity but do not affect ssDNA binding

The ability of the Q254 mutants to bind ssDNA was investigated using the electrophoretic mobility shift assay technique. The wild-type and all of the mutant proteins had a similar affinity (within a 2-fold difference) for ssDNA (Fig. 6).

Despite binding ssDNA normally, the ssDNA-dependent ATPase activity of all of the Q254 mutants was impaired by between 9- and 100-fold relative to wild-type (Table 1). The magnitude of the k_{cat} reduction was related to the nature of the residue at position 254. Poorest k_{cat} values were associated with the positively charged and polar Q254R, Q254N and Q254K mutants, then the neutral Q254A mutant, and the highest k_{cat} value was displayed by the negatively charged Q254E mutant.

With the exception of Q254K and Q254R, all Q254 mutants displayed reduced K_m values, most notably Q254A (30-fold decrease).

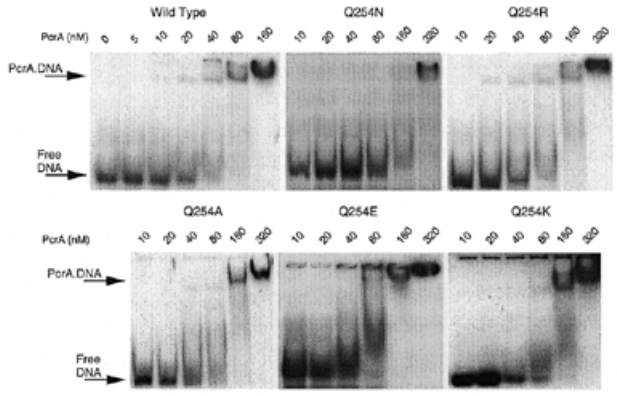

Figure 6. Electrophoretic mobility shift assays for wild-type PcrA and all Q254 mutants. Protein at various concentrations (indicated above each lane) was incubated with 2.5 nM single-stranded 45mer. Bound and free DNA were separated by electrophoresis through a 10% non-denaturing polyacrylamide gel. Experimental details are described in Materials and Methods.

The helicase activities of Q254 mutants are related to charge

All mutations at the Q254 residue reduced helicase activity substantially with respect to wild-type (Fig. 7). The magnitude of the decrease in activity was again related to the nature of the mutant residue. However, this time the trend we observed was opposite to that for the ATPase assays. Least affected were the positively charged Q254K and Q254R mutants and then the polar Q254N residue. Most affected were the neutral and negatively charged Q254A and Q254E mutants, which both displayed very low helicase activity.

DISCUSSION

It is a general requirement in all helicases, as well as in members of diverse groups of NTPases, to couple the free energy of nucleotide hydrolysis to conformational changes essential for enzyme function. We have studied how this is achieved in PcrA helicase by mutagenesis of motif III. Our results demonstrate that the motif III loop fulfils the dual role of both interacting with the nucleotide binding pocket and forming part of the DNA binding apparatus, which is responsible for separating DNA duplexes.

Motif III is involved in direct DNA interactions which are critical for helicase activity

The crystal structures of *E.coli* Rep helicase bound to ssDNA and ADP (10) and the 'substrate' and 'product' complexes of PcrA (7) reveal that the neighbouring tryptophan and arginine residues of motif III make direct contacts with the bound ssDNA. The motif III DNA binding site is involved in forming one of several 'pockets' which form a channel across the top of domains 1A and 2A. Here, bases of ssDNA are bound via aromatic stacking interactions and it is suggested that ssDNA translocation is the result of coordinated base flipping between these pockets (7). Biochemical evidence that the conserved tryptophan is involved in DNA binding comes from fluorescence quenching experiments in Rep (18) and now also from the W259A PcrA mutant. This mutation severely decreases the DNA binding affinity of the protein which now requires a 200-fold

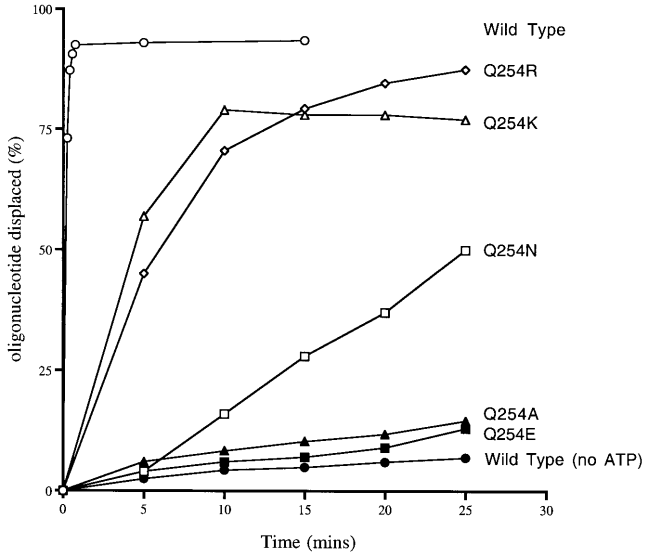

Figure 7. Helicase time course assays for wild-type PcrA (open circle), Q254K (open triangle), Q254R (open diamond), Q254N (open square), Q254A (filled triangle) and Q254E (filled square). A control assay for wild-type PcrA in the absence of ATP is also shown (filled circle). Reactions were performed with 0.6 μM protein and 1 nM DNA substrate. Annealed and displaced oligonucleotides were separated by electrophoresis through a 10% non-denaturing polyacrylamide gel and quantified using a phosphorimager and ImageQuant software (Molecular Dynamics).

higher concentration of ssDNA cofactor than the wild-type protein in order to achieve half-maximal stimulation of its ATPase activity (Fig. 3 and Table 1). In addition, the DNA binding defect of the mutant protein was readily detectable by dot blot and gel shift assays (Fig. 4A and B). However, its k_{cat} and K_m values for ATP hydrolysis are similar to those of the wild-type protein (Table 1). It appears, therefore, that W259 in motif III contributes significantly to the binding of ssDNA but plays no direct role in ATP hydrolysis. In contrast, mutation of the neighbouring arginine to alanine (R260A) resulted in a mutant protein which apparently showed only a mild defect in DNA binding (Figs 3 and 4). This defect was insufficient to be detected clearly by dot blot or gel shift assays (Fig. 4A and B) but could be observed by the effect of varying the concentration of the ssDNA cofactor in the ATPase assays (Fig. 3). This method suggests that the R260A mutation has decreased the ssDNA binding affinity of the protein only marginally (3.5-fold; Table 1). R260A mutant k_{cat} and K_m values for ATP hydrolysis are also similar to those of the wild-type protein (both 2-fold decreased). However, the helicase activity of the R260A protein (Fig. 5A) is reduced disproportionately (i.e. uncoupled) from the ATPase and DNA binding activities (around 90-fold). This observation could be explained if the conserved arginine of motif III is involved in stabilising energetically unfavourable DNA conformations during the strand separation reaction. Since the helicase activity of the W259A mutant (Fig. 5A) was also extremely low (despite normal ATPase kinetics) the tryptophan residue is clearly essential for the function of the enzyme. However, in this case it is more difficult to distinguish whether it is involved purely in binding DNA or whether it plays a more crucial role in the actual mechanism of strand separation. Nonetheless, even at very high concentrations of protein, the W259A mutant shows no significant helicase activity (Fig. 5B), highlighting the critical importance of the conserved tryptophan in wild-type PcrA.

The role of Q254 of motif III at the nucleotide binding pocket

The crystal structure of the *B.stearothermophilus* DNA helicase PcrA, with and without ADP (6), gave us insights into the possible coupling mechanism of the ATPase and helicase functions. Subdomains 1A and 2A of PcrA were found to be structurally homologous to the ATP binding domain of the recombination protein RecA. The structural homology is extended into the ATP binding pocket, where important amino acid residues involved in the binding and hydrolysis of ATP show a high degree of spatial conservation (Fig. 2A). This implies that PcrA and RecA may share similarities in their reaction mechanisms. The structures of both enzymes reveal the projection of the side chain of a conserved glutamine residue (Q194 and Q254 in RecA and PcrA, respectively) towards the space which is likely to be occupied by the γ-phosphate of bound ATP (6,11; Fig. 2A). Gln194 of RecA and Gln254 of PcrA are located at the end of loop L2 and the motif III loop, respectively, which are themselves structurally equivalent and are both involved in DNA binding interactions (discussed above; see also 11,19,20). On the basis of structural comparisons with the switch II region of ras p21, Story and Steitz (11) have suggested that Q194 is responsible for coupling ATP hydrolysis and DNA binding by interacting with the γ-phosphate of ATP and stabilising a high affinity binding state for ssDNA in loop L2. This proposal is supported by recent mutagenesis studies on Q194 of RecA (13), in which mutations at position 194 prohibited the formation of the high affinity binding state when ATPγS is bound. A similar role for Q254 in PcrA is suggested by recent structural studies. The 'substrate' and 'product' complexes of PcrA show how the Q254 residue does indeed contact the γ-phosphate before and after ATP hydrolysis (7; Fig. 1).

These considerations suggest an allosteric mechanism for PcrA (shown in Fig. 2B) in which Q254 plays a key role in coupling ATPase and helicase activities. To test the model we targeted this residue by site-directed mutagenesis and introduced a wide range of alterations in order to study the effects of residue size and charge on ATPase and helicase activities. All mutations at the Q254 position had deleterious effects on both ATPase and helicase rates, signalling the important role of residue 254 in both activities. None of the mutations at the Q254 position affected ssDNA binding significantly (Fig. 6). In our ATPase assays, although we generally observed severe k_{cat} reductions, some of the mutations at Q254 (notably Q254A) also produced enzymes with K_m decreases (Table 1). However, since the kinetic mechanism of ATP hydrolysis in PcrA is unknown, it is impossible to assess the significance of these K_m decreases. They may be related to an increased affinity for ATP or, more likely, are linked to changes in rate constants associated with conformational changes or product release. It may be of significance then that the only two mutations for which K_m was maintained at wild-type levels (Q254K/R) were also those for which helicase activity was highest (see below). On measuring k_{cat}, we observed a trend between the nature of the residue at position 254 and the magnitude of the

decrease relative to wild-type. Introducing a positive charge at this position (Q254K/R) seems to have a more severe effect on ATPase activity than introducing a negative charge (Q254E) (Table 1). Interestingly, the opposite is true with respect to the helicase activities, where the introduction of negative charge affects the helicase activity more severely than the introduction of positive charge (Fig. 7). This observation implies that there are altered levels of coupling between ATPase and helicase activities depending on the nature of the residue at the Q254 position. An amino acid residue with a positively charged side chain (which could interact with the γ-phosphate of the bound nucleotide) apparently results in better coupling of ATPase and helicase activities than one with a negatively charged side chain, which results in inefficient coupling of activities. For instance, although the Q254E mutant protein has between a 4- and 11-fold higher k_{cat} for ATP hydrolysis than the Q254K and Q254R proteins, its helicase activity is much lower (almost 0) by comparison. These experiments lead us to the proposal that Q254 acts as a γ-phosphate sensor. This suggestion is also consistent with the properties of the Q254A and Q254N mutant proteins. The Q254A mutation, like Q254E, abolishes the γ-phosphate sensor ability of the protein and causes uncoupling of ATPase and helicase activities. The Q254N mutation appears to display an intermediate level of coupling, probably because the shorter polar side chain of asparagine results in poor γ-phosphate sensor ability. This mutation suggests that residue size also affects the coupling mechanism. However, in being better at coupling ATPase and helicase activities than the larger glutamate residue, it also confirms that charge plays a critical role.

Nature has selected a polar glutamine to fulfil the role of γ-phosphate sensor in wild-type PcrA rather than a positively charged residue (such as lysine). This can be rationalised in the light of the undesirably low rates of ATP hydrolysis displayed by Q254K and Q254R mutants (Table 1). Perhaps introduction of positive charge near the γ-phosphate of ATP interferes with activation of the water molecule required for in-line attack or results in slow product release. The effective helicase activity of the wild-type protein may therefore be thought of as a compromise between efficient ATP hydrolysis and efficient coupling of this activity to DNA strand separation.

The mechanism for coupling ATPase to helicase activity seems to be sensitive both to the position and charge of the side chain of the amino acid residue at the 254 position in motif III. Both of these factors may be influenced transiently in the wild-type protein as the enzyme passes through cycles of ATP binding and hydrolysis. In line with the model presented in Figure 2B, we propose that this 'switch' forms a part of the mechanism of communication between ATP binding and DNA binding sites in PcrA and superfamily I DNA helicases in general. Other motifs are also likely to play a role in this complex process. For instance, Hall *et al.* (21) and Soultanas *et al.* (22) propose that motif VI of superfamily I helicases is also involved in the coupling activity.

This energy coupling mechanism appears to be conserved between PcrA helicase and RecA, but analogous 'switches' also exist in other NTP-hydrolysing enzymes. For instance, ras p21 and Ef-tu, the archetypal molecular switch proteins, contain switches that are structurally similar to that found in RecA (11), but which employ backbone amides rather than a conserved glutamine as the γ-phosphate sensor (12,23,24). It seems likely that this theme will extend to further members of the diverse groups of NTP-utilising enzymes.

ACKNOWLEDGEMENTS

We wish to thank Val Cooper for oligonucleotide synthesis, Amarjit Bhomra for DNA sequencing and Jennifer Byrne for technical assistance. This work was supported by the Wellcome Trust.

REFERENCES

1. Lohman,T.M. and Bjornson,K.P. (1996) *Annu. Rev. Biochem.*, **65**, 169–214.
2. Bird,L.E., Subramanya,H.S. and Wigley,D.B. (1998) *Curr. Opin. Struct. Biol.*, **8**, 14–18.
3. Wong,I. and Lohman,T.M. (1992) *Science*, **256**, 350–355.
4. Iordanescu,S. (1993) *Mol. Gen. Genet.*, **241**, 185–192.
5. Bird,L.E., Brannigan,J.A., Subramanya,H.S. and Wigley,D.B. (1998) *Nucleic Acids Res.*, **26**, 2686–2693.
6. Subramanya,H.S., Bird,L.E., Brannigan,J.A. and Wigley,D.B. (1996) *Nature*, **384**, 379–383.
7. Velankar,S., Soultanas,P., Dillingham,M.S., Subramanya,H.S. and Wigley,D.B. (1999) *Cell*, **97**, 75–84.
8. Brosh,R.M.,Jr and Matson,S.W. (1996) *J. Biol. Chem.*, **271**, 25360–25368.
9. Brosh,R.M.,Jr and Matson,S.W. (1997) *J. Biol. Chem.*, **272**, 572–579.
10. Korolev,S., Hsieh,J., Gauss,G.H., Lohman,T.M. and Waksman,G. (1997) *Cell*, **90**, 635–647.
11. Story,R.M. and Steitz,T.A. (1992) *Nature*, **355**, 374–376.
12. Milburn,M.V., Tong,L., DeVos,A.M., Brünger,A., Yamaizumi,Z., Nishimura,S. and Kim,S.-H. (1990) *Science*, **247**, 939–945.
13. Kelley,J.A. and Knight,K.L. (1997) *J. Biol. Chem.*, **272**, 25778–25782.
14. Clackson,T., Güssow,D. and Jones,P.T. (1991) In McPherson,M.J., Quirke,P. and Taylor,G.R. (eds) *PCR—A Practical Approach*. IRL Press, Oxford, UK, pp. 207–209.
15. Soultanas,P., Dillingham,M.S. and Wigley,D.B. (1998) *Nucleic Acids Res.*, **26**, 2374–2379.
16. Pullman,M.E., Penefsky,H.S., Datta,A. and Racker,E. (1960) *J. Biol. Chem.*, **235**, 3322–3329.
17. Crute,J.J., Mocarski,E.S. and Lehman,I.R. (1988) *Nucleic Acids Res.*, **16**, 6585–6596.
18. Bjornson,K.P., Moore,K.J.M. and Lohman,T.M. (1996) *Biochemistry*, **35**, 2268–2282.
19. Malkov,V.A. and Camerini-Otero,R.D. (1995) *J. Biol. Chem.*, **270**, 30230–30233.
20. Voloshin,O.N., Wang,L. and Camerini-Otero,R.D. (1996) *Science*, **272**, 868–872.
21. Hall,M.C., Özsoy,A.Z. and Matson,S.W. (1998) *J. Mol. Biol.*, **277**, 257–271.
22. Soultanas,P., Dillingham,M.S., Velankar,S.S. and Wigley,D.B. (1999) *J. Mol. Biol.*, **290**, 137–148.
23. Berchtold,H., Reshetnikova,L., Reiser,C.O.A., Schirmer,N.K., Sprinzl,M. and Hilgenfeld,R. (1993) *Nature*, **365**, 126–132.
24. Bourne,H.R., Sanders,D.A. and McCormick,F. (1991) *Nature*, **349**, 117–127.